

AD-A231 607

DOCUMENTATION PAGE

Form Approved
OAS No. 6704-0100

1a. REPORT SECURITY CLASSIFICATION UNCLASSIFIED		1b. RESTRICTIVE MARKINGS	
2a. SECURITY PROCESSING AUTHORITY DTIC		3. DISTRIBUTION/AVAILABILITY OF REPORT <i>Approved for public release; distribution unlimited</i>	
2b. DECLASSIFICATION/DOWNGRADING SCHEDULE SELECTED FEB 15 1991		5. MONITORING ORGANIZATION REPORT NUMBER(S) AFOSR-TR- 91 0027	
4. PERFORMING ORGANIZATION REPORT NUMBER(S) CLS-90-101		7a. NAME OF MONITORING ORGANIZATION <i>Same as 6a</i>	
6a. NAME OF PERFORMING ORGANIZATION University of Southern California	6b. OFFICE SYMBOL (if applicable)	7b. ADDRESS (City, State, and ZIP Code) <i>Same as 6a</i>	
6c. ADDRESS (City, State, and ZIP Code) Center for Laser Studies Los Angeles, CA 90089-1112		9. PROCUREMENT INSTRUMENT IDENTIFICATION NUMBER AFOSR-88-0038	
8a. NAME OF FUNDING/SPONSORING ORGANIZATION AFOSR	8b. OFFICE SYMBOL (if applicable) <i>NE</i>	10. SOURCE OF FUNDING NUMBERS	
8c. ADDRESS (City, State, and ZIP Code) Bolling Air Force Base, DC 20332		PROGRAM ELEMENT NO. <i>61102</i>	PROJECT NO. <i>2306</i>
		TASK NO. <i>B1</i>	WORK UNIT ACCESSION NO.
11. TITLE (Include Security Classification) Thermal Transport Studies of Optical Coatings, Interfaces and Surfaces by Thermal Diffusion-Wave Interferometry			
12. PERSONAL AUTHOR(S) Randall T. Swimm			
13a. TYPE OF REPORT Final Technical	13b. TIME COVERED FROM 12/1/87 TO 6/30/90	14. DATE OF REPORT (Year, Month, Day) 1990, Aug. 6	15. PAGE COUNT 12
16. SUPPLEMENTARY NOTATION			
17. COSATI CODES		18. SUBJECT TERMS (Continue on reverse if necessary and identify by block number)	
FIELD	GROUP	SUB-GROUP	
		Optical Coatings, Thermal Transport	
19. ABSTRACT (Continue on reverse if necessary and identify by block number)			
<p>Thermal diffusion-wave interferometry can produce a wealth of thermal transport information on a single sample. Onset of three-dimensional heat flow, contributions due to thermal contact resistance, evidence of transit time effects, and the presence of unanticipated stratified layers are some of the phenomena that may be seen. The natural consequence of the observed sensitivity to the detailed transport physics is that great care must be taken when interpreting the data. However, the revealed detail ensures that essential effects are not overlooked.</p>			
20. DISTRIBUTION/AVAILABILITY OF ABSTRACT <input checked="" type="checkbox"/> UNCLASSIFIED/UNLIMITED <input type="checkbox"/> SAME AS RPT. <input type="checkbox"/> DTIC USERS		21. ABSTRACT SECURITY CLASSIFICATION UNCLASSIFIED	
22a. NAME OF RESPONSIBLE INDIVIDUAL <i>P. M. Swimm</i>		22b. TELEPHONE (Include Area Code) <i>202-717-4931</i>	22c. OFFICE SYMBOL <i>NE</i>

Report CLS-90-101

**Thermal Transport Studies of Optical Coatings, Interfaces
and Surfaces by Thermal Diffusion-Wave Interferometry**

Randall T. Swimm, Principal Investigator
Center for Laser Studies
University of Southern California
Los Angeles, CA 90089-1112

6 August 1990

Final Technical Report

Contract Number AFOSR-88-0038

Prepared for:
Air Force Office of Scientific Research
Bolling Air Force Base, DC 20332

Table of Contents

	Page
Research Objectives	1
Research Status	1
Publications	1
Participating Professionals	1
Oral Presentations	2
Discoveries, Inventions, Patents	2
Appendix I	3



Accession For	
NTIS GRA&I	<input checked="" type="checkbox"/>
DTIC TAB	<input type="checkbox"/>
Unannounced	<input type="checkbox"/>
Justification _____	
By _____	
Distribution/ _____	
Availability Codes	
Dist	Avail and/or Special
A-1	

Research Objectives

- (1) Complete the development of a measurement system designed to determine the thermal transport properties of single samples of either zero, one or two coating layers deposited on a substrate.
- (2) Measure the thermal transport properties of uncoated metal mirrors.
- (3) Measure the thermal transport properties of single-layer metal coatings.
- (4) Measure the thermal transport properties of two-layer coating stacks consisting of a dielectric layer covered by a metal layer.

Research Status

Objectives 1-3 were successfully completed. Objective 4 was not completed. Appendix I contains a preprint that presents a comprehensive summary of the research results obtained under the present AFOSR grant.

Publications

The principal investigator expects to submit a paper describing the currently funded research to Applied Physics Letters. The probable title is: "Thermal Transport Studies of Optical Coatings, Interfaces, and Surfaces." The anticipated author list includes the principal investigator and Gary Wiemokly.

Participating Professionals

This research was carried out jointly by the principal investigator and Gary Wiemokly, a former graduate student at the University of Southern California.

Oral Presentations

"Thermal Transport Studies of Optical Coatings, Interfaces and Surfaces by Thermal Diffusion Wave Interferometry", Randall T. Swimm and Gary Wiemokly, presented at the 1989 Boulder Damage Symposium, held Nov. 1-3, 1989 in Boulder, Colorado. Appendix I contains a preprint of the paper submitted to the conference proceedings, to appear under the title: Laser Induced Damage in Optical Materials: 1989.

Discoveries, Inventions, Patents

No discoveries, inventions or patents are reported.

Thermal Transport Studies of Optical Coatings, Interfaces and Surfaces by Thermal Diffusion Wave Interferometry

Randall T. Swimm and Gary Wiemokly
Center for Laser Studies
University of Southern California
Los Angeles, CA 90089-1112

Thermal transport data on thin metal coatings are presented. The data illustrate the ability of the measurement technique to characterize the thermal transport properties of single samples. The method offers insight on coating survivability.

key words: adhesion; coatings; damage; delamination; laser hardness; laser-induced damage; nondestructive evaluation; nuclear hardness; optical coatings; thermal conductivity; thermal diffusivity; thermal properties; thermal transport; thin films.

Introduction

The unifying characteristic of thin-film coating studies is the need to separate the surface and interface properties of the coating from the bulk properties of the coating. Frequently this separation is accomplished by varying a characteristic length of the system. Methods of doing so fall into at least two classes. The first class of measurement methods is based on varying the sample thickness. By plotting the measured value of an appropriately chosen property of the samples as a function of sample thickness, the sum of the surface and interface contributions may be extracted as the ordinate intercept of the data at zero thickness, and the bulk contribution may be obtained as the slope or the reciprocal of the slope of the data. A tacit assumption of this approach is that the sample properties are independent of coating thickness. An additional requirement is that the material properties be repeatable among samples. Finally, the signal to noise ratio and the data reproducibility must be adequate. In practice, it may be difficult to satisfy all of these conditions, especially with regard to material properties repeatability. As a consequence, data are occasionally reported which show nonphysical results such as negative slopes or negative intercepts. Unless the substrate polishing and coating deposition processes are under sufficient control to yield repeatable coating properties, the attempt to obtain meaningful results by utilizing measurement techniques based on multiple samples of different coating thickness is futile.

An alternative class of measurement methods is based on varying a characteristic length imposed by the measurement process, and obtaining separate surface, bulk and interface contributions for a single coated sample. Such techniques may include those based on varying a spot size, the physical offset between pumped and probed regions, a wavelength or a diffusion length. The present work falls into this latter class of measurement methods. The goal of this paper is to show that a great deal may be learned about the thermal transport properties of a single sample.

Background

The measurement and analysis techniques have been described in earlier proceedings^{1,2}. Briefly, the physics of the measurement is as follows. Under steady-state conditions of sinusoidally modulated surface heating, thermal waves generated at the sample surface diffuse through the sample and partially reflect at abrupt discontinuities of the thermal effusivity (equal to the thermal conductivity divided by the square root of the thermal diffusivity³). Reflected thermal waves that return to the sample surface interfere with the instantaneous thermal waves being generated at the surface, causing the surface temperature response to be out of phase with the response that would occur in the absence of reflected thermal waves. In the present work, a metal coating or a bare metal substrate is used to ensure the required condition that the thermal waves be generated in a depth that is small compared to the local thermal diffusion length in order to preserve interference contrast. The thermal waves are generated by heating the sample using a sinusoidally-modulated argon ion laser beam. The temperature response is detected using an unmodulated helium neon laser beam reflected from the center of the heated region, based on the fact that the metal reflectivity is temperature dependent. The weak intensity modulation induced on the HeNe laser beam is measured using a silicon detector and lock-in detection. The system electronic phase is separately calibrated by directing the pump beam into the probe detector. The measured phase of the temperature response constitutes the data. The data are modelled using the boundary value solution for the presumed sample structure, in which the material properties are included as adjustable parameters. In the present modelling, the piecewise constant approximation is used, and the thermal contact resistance is included. A key consideration is the uniqueness of the solution. This can be inferred only by individually studying a sufficient range of different sample types so as to exclude alternative possibilities.

The present measurement system is an upgraded version of that described in the earlier proceedings^{1,2}. A Coherent, Inc. model 90-6 Innova argon ion laser is used as the pump laser. A second probe beam line has been added to allow the temperature response at the coating-to-substrate interface to be determined for samples with a transparent substrate. Various other refinements have been added to avoid systematic errors. These include improved detector shielding, optical baffling to minimize light scattered into the detectors, and careful optical alignment to avoid stray reflections. A custom-built Lasermetrics, Inc. electro-optic modulator with reduced crystal spacing is used to avoid thermal lensing in the index matching fluid at high pump-beam power (3 W at 514.5 nm). Data are recorded using an automated system.

Recent related work by other authors is listed in the references⁴⁻¹¹.

Results and Discussion

Results for a 1 μm rf sputtered Ni coating deposited on fused silica are presented in Fig. 1. The sample was sinusoidally heated at the coating surface. The phase of the sinusoidal temperature response is plotted as a function of the logarithm of the modulation frequency. The circles show the response at the coating surface. The squares show the response at the coating-to-substrate interface. The upper curve shows the results of a zero-parameter fit (i.e. no adjustable parameters), based on a one-dimensional heat flow model assuming the handbook values for thermal conductivity and thermal diffusivity of Ni in bulk format, and also assuming a thermal contact resistance equal to zero. The

lower curve shows the theoretical response at the interface under identical assumptions. Several conclusions may be drawn from the data and the model agreement.

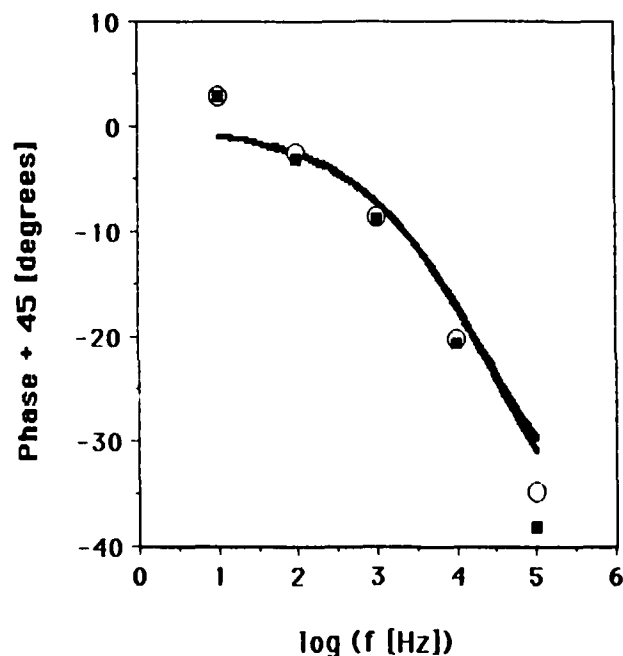


Fig. 1. 1 μm RF Sputtered Ni Coating on Fused Silica

First consider the near-equality of the surface and interface data at low modulation frequencies. The phase of the temperature response at the surface and the interface is expected to be equal at modulation frequencies for which the coating thickness is much less than the thermal diffusion length in the coating. The observed near-equality is a strong indicator of whether the data are due to the temperature modulation of the coating reflectance as assumed. Because of the small values typical of the thermal coefficient of the reflectance, numerous synchronous background signals giving rise to systematic errors had to be eliminated before the observed agreement of surface and interface response was attained.

Attempts to fully account for the data in terms of a one-dimensional heat flow model with a non-zero thermal contact resistance failed. However, the one-dimensional model is known to fail at frequencies for which the thermal diffusion length is not small compared to the pump spot diameter. The tentative interpretation of the data is that the Ni coating is displaying essentially bulk-like thermal transport behavior, with negligible thermal contact resistance, and with three-dimensional heat flow exhibited at low modulation frequencies. In order to verify the signature of three-dimensional heat flow in the simplest possible case, a solid metal mirror was studied.

Results for a solid Mo mirror, using a 1.90 mm diameter gaussian pump spot are considered next. The surface of the mirror was visibly oxidized. Mo is known to form sub-oxide surface layers several hundred angstroms thick¹². The model calculation assumes no oxide layer, and uses hand-book values for the Mo thermal transport parameters. The theoretical derivation follows that of Carslaw and Jaeger¹³, except that the temporally modulated gaussian pump intensity distribution is used for the heat flux instead of a constant flux over a circular region as treated by Carslaw and

Jaeger. Consider the cylindrically symmetric heat diffusion equation for a homogeneous isotropic medium (assuming small temperature excursions, and therefore ignoring temperature dependence of thermal transport coefficients), for the region $z \geq 0$

$$\frac{\partial^2 T}{\partial r^2} + \frac{\partial^2 T}{\partial z^2} - \frac{1}{\kappa} \frac{\partial T}{\partial t} = 0 \quad (1)$$

where T equals temperature, κ equals thermal diffusivity, z equals depth, r equals radial distance and t equals time. For a solution of the form $T = T e^{i\omega t}$, where T is temperature amplitude, i is the square root of minus one and ω is angular frequency, a Fourier transform yields the steady-state equation:

$$\frac{\partial^2 T}{\partial r^2} + \frac{\partial^2 T}{\partial z^2} - \frac{i\omega}{\kappa} T = 0. \quad (2)$$

For a gaussian pump beam, Eq. (2) is to be solved subject to the following boundary conditions:

$$-K \left[\frac{\partial T}{\partial z} \right]_{z=0} = I_0 e^{-2\left(\frac{r}{r_0}\right)^2}, \quad (3)$$

where K equals thermal conductivity, I_0 equals intensity and r_0 equals the $1/e^2$ radius of the pump beam. Applying a Hankel transform of order zero to Eq. (2) yields the equation:

$$\frac{d^2 V_0}{dz^2} - \sigma^2 V_0 - \frac{i\omega}{\kappa} V_0 = 0 \quad (4)$$

where

$$V_0 = \int_0^\infty r T(r,z) J_0(\sigma r) dr. \quad (5)$$

and σ is the transform variable conjugate to r . Eq. (4) is subject to the following transformed boundary conditions.

$$-K \left[\frac{\partial V_0}{\partial z} \right]_{z=0} = I_0 \int_0^\infty r e^{-2\left(\frac{r}{r_0}\right)^2} J_0(\sigma r) dr \quad (6)$$

It follows by inspection that the following is a solution to Eq. (4), subject to Eq. (6) and vanishing as $z \rightarrow \infty$

$$V_0 = \frac{I_0}{K} \int_0^\infty r e^{-2\left(\frac{r}{r_0}\right)^2} J_0(\sigma r) dr \frac{e^{-\sqrt{\sigma^2 + \frac{i\omega}{\kappa}} z}}{\sqrt{\sigma^2 + \frac{i\omega}{\kappa}}}. \quad (7)$$

and therefore by inversion that the following is a solution to Eq. (2), subject to Eq. (3) and vanishing as $z \rightarrow \infty$.

$$T = \frac{I_0}{K} \int_0^\infty \int_0^\infty r e^{-2\left(\frac{r}{r_0}\right)^2} J_0(\sigma r) dr \frac{e^{-\sqrt{\sigma^2 + \frac{i\omega}{\kappa}} z}}{\sqrt{\sigma^2 + \frac{i\omega}{\kappa}}} \sigma J_0(\sigma r) d\sigma \quad (8)$$

This integral may be simplified as follows¹⁴.

$$T(r,z) = \frac{r_0^2 I_0}{4K} \int_0^\infty \frac{\sigma}{\sqrt{\sigma^2 + \frac{i\omega}{\kappa}}} e^{-\frac{\sigma^2 r_0^2}{8}} e^{-\sqrt{\sigma^2 + \frac{i\omega}{\kappa}} z} J_0(\sigma r) d\sigma. \quad (9)$$

Eq. (9) expresses the temperature at a general point in a semi-infinite solid with gaussian heating at the surface. In the experiments, the temperature is measured at the center of the heated spot. Therefore, the point of interest has coordinates $r=0$, $z=0$. Consequently, the temperature response simplifies to the following expression (after converting the integral to dimensionless variables)¹⁵:

$$T \Big|_{\substack{r=0 \\ z=0}} = \frac{r_0^2 I_0}{4K} \sqrt{\frac{\omega}{\kappa}} \int_0^\infty \frac{s}{\sqrt{s^2 + i}} e^{-b^2 s^2} ds, \quad (10)$$

where $s = \sigma\sqrt{\kappa/\omega}$, and $b = (r_0/2)\sqrt{\omega/2\kappa}$. The phase ϕ of the temperature response relative to the sinusoidal pump-beam modulation may be obtained as the arctangent of the quotient of the imaginary component divided by the real component, as follows.

$$\phi(\kappa, r_0; \omega) \Big|_{\substack{r=0 \\ z=0}} = \tan^{-1} \left\{ (-) \frac{\int_0^\infty \frac{s}{\sqrt{s^2 + i}} \sqrt{1 - \left[\frac{s}{\sqrt{s^2 + i}} \right]^2} e^{-b^2 s^2} ds}{\int_0^\infty \frac{s}{\sqrt{s^2 + i}} \sqrt{1 + \left[\frac{s}{\sqrt{s^2 + i}} \right]^2} e^{-b^2 s^2} ds} \right\} \quad (11)$$

Calculations based on this expression (with no adjustable parameters) are presented in Fig. 2.

Reference to Fig. 2 shows that most of the measured phase variation is accounted for by the model. On the basis of one-dimensional calculations, the departure of the data from the model is con-

sistent with that expected, due to the presence of the surface oxide layer. The form of the three-dimensional numerical calculations also supports the hypothesis that the low-frequency departure of the measured phase from the one-dimensional model presented in Fig. 1 is due to the onset of three-dimensional heat flow.

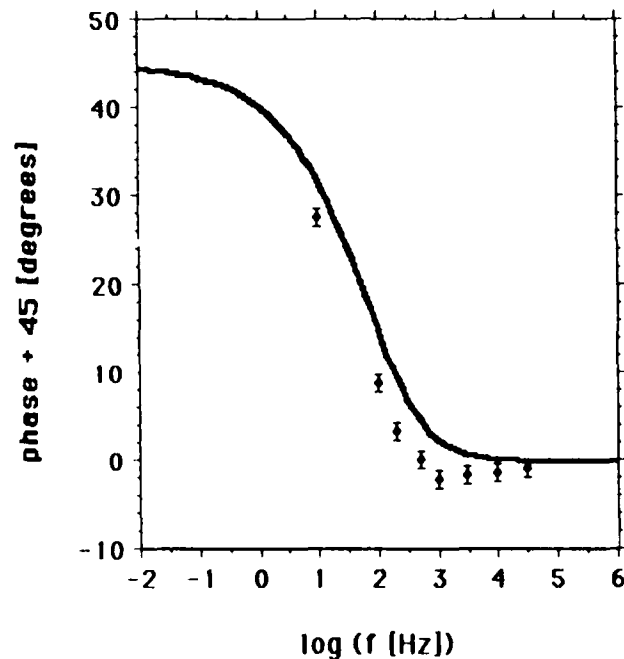


Fig. 2. Solid Mo Mirror

In an effort to obtain data free from three-dimensional heat flow effects, a metal coating of lower thermal diffusivity was studied. Results for a 1 μm rf sputtered Ti coating deposited on fused silica are presented in Fig. 3. The phase of the sinusoidal temperature response is plotted as a function of the logarithm of the modulation frequency. The circles show the response at the coating surface. The squares show the response at the coating-to-substrate interface. The upper curve shows the results of a zero-parameter fit (i.e. no adjustable parameters), based on a one-dimensional heat flow model assuming the handbook values for thermal conductivity and thermal diffusivity of Ti in bulk format, and also assuming a thermal contact resistance equal to zero. The lower curve shows the theoretical response at the interface under identical assumptions.

The near equality of the of the surface and interface data at low modulation frequencies again confirms the absence of a large class of potential systematic errors. Note also that the low modulation frequency data are in agreement with the one-dimensional heat flow model calculations. The gradual increase of the phase difference between the temperature response at the surface and the interface is expected, on the basis of thermal transit-time effects. The agreement of the experimental and theoretical differences between surface and interface response per se is fair. Unfortunately, the data show additional, unexpected structure in the modulation-frequency range above 10 kHz. The authors originally suspected that this structure may have been due to the presence of an additional stratified layer with an abrupt interface. Possible explanations in terms of a thermally-thick interface layer, a coating surface oxide layer, and a sub-surface substrate polishing damage layer were all examined via modelling. However, additional measurements were performed on a number of samples, including a

coating e beam deposited onto a sapphire substrate, a Ti coating dc magnetron sputtered on to a fused silica substrate that had been argon-ion beam milled after polishing to remove a graded layer two to

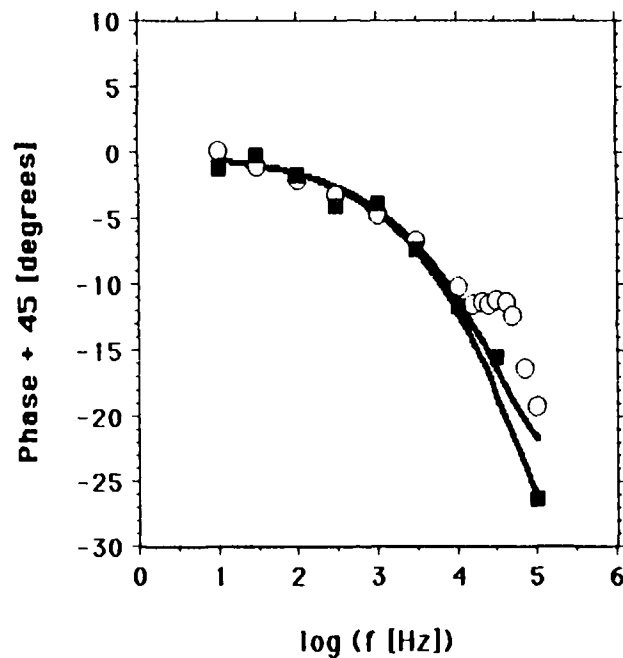


Fig. 3. 1 μ m RF Sputtered Ti Coating on Fused Silica

ten micrometers thick¹⁶, and the Mo mirror at a finer grid of modulation frequencies. In every case, structure was observed in the same modulation frequency interval. Since the unexplained data structure occurs at the same modulation frequency in many dissimilar samples, it is quite likely to be the result of a systematic error. Further work to identify the cause is under way. Notwithstanding the presence of the unexplained structure, the tentative interpretation of the data is that the Ti coating is displaying essentially bulk-like thermal transport behavior, with negligible thermal contact resistance (much less than 10^{-2} K/(W/cm²)), and with one-dimensional heat flow exhibited at all modulation frequencies employed.

Conclusion

Thermal-wave interferometry can produce a wealth of thermal transport information on a single sample. Onset of three-dimensional heat flow, contributions due to thermal contact resistance, evidence of transit time effects, and the presence of unanticipated stratified layers are some of the phenomena that may be seen. As the preceding results imply, the present agreement with plausible models based on handbook transport data suggests that quantitative modelling using adjustable parameters should also be possible, provided that the physical origin of the observed data is understood. The natural consequence of the sensitivity to the detailed transport physics that is shown is that great care must be taken while interpreting the data. However, the revealed detail ensures that essential effects are not overlooked.

Acknowledgments

Productive discussions with Alan Stewart (Battelle PNL), Kent Stowell (Weapons Laboratory) and Patricia White (Battelle PNL) are gratefully acknowledged. This research was funded by grant AFOSR-88-0038 from the Air Force Office of Scientific Research.

- ¹R.T. Swimm and L. Hou, NIST Special Publication 752, Laser Induced Damage in Optical Materials: 1986 (Government Printing Office, Washington, DC, 1988), p. 251.
- ²R.T. Swimm, NIST Special Publication 756, Laser Induced Damage in Optical Materials: 1987 (Government Printing Office, Washington, DC, 1988), p.328.
- ³R.T. Swimm, Appl. Phys. Lett. **42**, 955 (1983).
- ⁴J. Baumann and R. Tilgner, J. Appl. Phys. **58**, 1982 (1985).
- ⁵C.A. Paddock and G.L. Eesley, J. Appl. Phys. **60**, 285 (1986).
- ⁶Akira Ono, Tetsuya Baba, Hiroyuki Funomoto and Akira Nishikawa, Jpn. J. Appl. Phys. **25**, L808 (1986).
- ⁷L.J. Bortner, R.S. Newrock and D.J. Resnick, J. Appl. Phys. **61**, 4452 (1987).
- ⁸E.T. Swartz and R.O. Pohl, Appl. Phys. Lett. **51**, 2200 (1987).
- ⁹B.M. Clemens, G.L. Eesley and C.A. Paddock, Phys. Rev. B **37**, 1085 (1988).
- ¹⁰H.P.R. Frederikse and X.T. Ying, Appl. Opt. **27**, 4672 (1988).
- ¹¹J.C. Lambropoulos, M.R. Jolly, C.A. Amsden, S.E. Gilman, M.J. Sinicropi, D. Diakomihalis and S.D. Jacobs, J. Appl. Phys. **66**, 4230 (1989).
- ¹²Ray Bell (Lockheed, Inc.), private communication.
- ¹³H.S. Carslaw and J.C. Jaeger, in Conduction of Heat in Solids (Oxford University Press, Oxford, 1959), Chap. XVII, p. 461.
- ¹⁴M. Abramowitz and I.A. Stegun (ed.), in Handbook of Mathematical Functions, U.S. Dept. of Commerce, Nat. Bur. of Stand., Appl. Math. Series **55** (Government Printing Office, Washington, DC, 1964), Eq. 11.4.29, p. 486.
- ¹⁵The $\exp(-\sigma^2 r_0^2/8)$ factor in the integrand of Eq.(9) keeps the integral and its derivatives with respect to r and z well behaved as $r \rightarrow 0$ and $z \rightarrow 0$.
- ¹⁶In collaboration with Patricia White.

Erratum

A systematic error that entered during the system phase calibration was discovered in the data presented in [2]. Consequently the data and data analysis in that paper are invalid.

Addendum

The peak in the data shown in fig. 3 was found to be due to a frequency-independent 2.5 degree error in the orthogonality of the in-phase and quadrature channels of the lock-in detector. The resultant error in the plotted difference data (signal phase minus calibration phase) shows a frequency dependence according to the actual values of the instrumental phase shift. The data may be corrected by a simple coordinate transformation. (8/21/90)